arXiv:hep-ph/0302092 v1   12 Feb 2003

The Neutrino Mass Window
for Baryogenesis

W. Buchmüller

Deutsches Elektronen-Synchrotron DESY, 22603 Hamburg, Germany

P. Di Bari

IFAE, Universitat Autònoma de Barcelona,

08193 Bellaterra (Barcelona), Spain

M. Plümacher

Theory Division, CERN, 1211 Geneva 23, Switzerland

Abstract

Interactions of heavy Majorana neutrinos in the thermal phase of the early universe may be the origin of the cosmological matter-antimatter asymmetry. This mechanism of baryogenesis implies stringent constraints on light and heavy Majorana neutrino masses. We derive an improved upper bound on the CP asymmetry in heavy neutrino decays which, together with the kinetic equations, yields an upper bound on all light neutrino masses of 0.1 eV. Lepton number changing processes at temperatures above the temperature T_B of baryogenesis can erase other, pre-existing contributions to the baryon asymmetry. We find that these washout processes become very efficient if the effective neutrino mass $\widetilde{m}_1$ is larger than $m_* \simeq 10^{-3}$ eV. All memory of the initial conditions is then erased. Hence, for neutrino masses in the range from $\sqrt{\Delta m_{\mathrm{sol}}^2} \simeq 8 \times 10^{-3}$ eV to $\sqrt{\Delta m_{\mathrm{atm}}^2} \simeq 5 \times 10^{-2}$ eV, which is suggested by neutrino oscillations, leptogenesis emerges as the unique source of the cosmological matter-antimatter asymmetry.
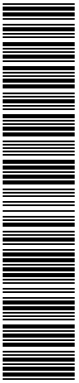
1 Introduction

The explanation of the cosmological baryon asymmetry is a challenge for particle physics and cosmology. In an expanding universe, which leads to departures from thermal equilibrium, C, CP and baryon number violating interactions of quarks and leptons can generate dynamically a baryon asymmetry [1]. The possible realization of these conditions has first been studied in detail in the context of grand unified theories [2, 3].

The picture of baryogenesis is significantly changed by the fact that already in the standard model of particle physics baryon (B) and lepton (L) number are not conserved due to quantum effects [4]. The corresponding non-perturbative $\Delta B = 3$ and $\Delta L = 3$ processes are strongly suppressed at zero temperature. However, at temperatures above the critical temperature T_{EW} of the electroweak transition they are in thermal equilibrium [5] and only the difference $B - L$ is effectively conserved.

During the past years data on atmospheric and solar neutrinos have provided strong evidence for neutrino masses and mixings. In the seesaw mechanism [6] the smallness of these neutrino masses m_ν is explained by the mixing m_D of the left-handed neutrinos with heavy Majorana neutrinos of mass M, which yields the light neutrino mass matrix

$$m_\nu = -m_D \frac{1}{M} m_D^T \ . \tag{1}$$

Since $m_D = \mathcal{O}(v)$, where $v \simeq 174$ GeV is the electroweak scale, and $M \gg v$, the neutrino masses m_ν are suppressed compared to quark and charged lepton masses. CP violating interactions of the heavy Majorana neutrinos can give rise to a lepton asymmetry and, via the $\Delta B = 3$ and $\Delta L = 3$ sphaleron processes, to a related baryon asymmetry. This is the simple and elegant leptogenesis mechanism [7].

Leptogenesis is a non-equilibrium process which takes place at temperatures $T \sim M_1$. For a decay width small compared to the Hubble parameter, $\Gamma_1(T) < H(T)$, heavy neutrinos are out of thermal equilibrium, otherwise they are in thermal equilibrium. A rough estimate of the borderline between the two regimes is given by $\Gamma_1 = H(M_1)$ (cf. [8]). This is equivalent to the condition that the effective neutrino mass $\widetilde{m}_1 = (m_D^\dagger m_D)_{11}/M_1$ equals the 'equilibrium neutrino mass'

$$m_* = \frac{16\pi^{5/2}}{3\sqrt{5}} g_*^{1/2} \frac{v^2}{M_{pl}} \simeq 10^{-3} \text{ eV} \ , \tag{2}$$

where we have used $M_{pl} = 1.2 \times 10^{19}$ GeV and $g_* = 434/4$ as effective number of degrees of freedom. For $\widetilde{m}_1 > m_*$ ($\widetilde{m}_1 < m_*$) the heavy neutrinos of type N_1 are in (out of) thermal equilibrium at $T = M_1$.

2

It is very remarkable that the equilibrium neutrino mass m_* is close to the neutrino masses suggested by neutrino oscillations, $\sqrt{\Delta m^2_{\rm sol}} \simeq 8 \times 10^{-3}$ eV and $\sqrt{\Delta m^2_{\rm atm}} \simeq 5 \times 10^{-2}$ eV. This suggests that it may be possible to understand the cosmological baryon asymmetry via leptogenesis as a process close to thermal equilibrium. Ideally, $\Delta L = 1$ and $\Delta L = 2$ processes would be strong enough at temperatures above M_1 to keep the heavy neutrinos in thermal equilibrium and weak enough to allow the generation of an asymmetry at temperatures below M_1.

An analysis of solutions of the Boltzmann equations shows that this is indeed the case if light and heavy neutrino masses lie in an appropriate mass range. In general, the final baryon asymmetry is the result of a competition between production processes and washout processes which tend to erase any generated asymmetry. Unless the heavy Majorana neutrinos are partially degenerate, $M_{2,3} - M_1 \leq M_1$, the dominant processes are decays and inverse decays of N_1 and the usual off-shell $\Delta L = 1$ and $\Delta L = 2$ scatterings. The final baryon asymmetry then depends on just four parameters [9] : the mass M_1 of N_1, the CP asymmetry ε_1 in N_1 decays, the effective neutrino mass $\widetilde{m}_1$ and, finally, the sum of all neutrino masses squared, $\overline{m}^2 = m_1^2 + m_2^2 + m_3^2$, which controls an important class of washout processes. Together with the two mass squared differences $\Delta m^2_{\rm atm}$ and $\Delta m^2_{\rm sol}$, the sum $\overline{m}^2$ determines all neutrino masses. Using an upper bound on the CP asymmetry ε_1 [10, 11], an upper bound on all light neutrino masses of 0.2 eV has recently been derived [12].

In this paper we extend the previous analysis in two directions. We derive an improved upper bound on the CP asymmetry which leads to a more stringent upper bound on light neutrino masses. In addition, we study in detail the washout of a pre-existing $B - L$ asymmetry, which yields a lower bound on the effective neutrino mass $\widetilde{m}_1$. In this way we obtain a window of neutrino masses for which leptogenesis can explain the observed cosmological baryon asymmetry, independent of initial conditions.

The paper is organized as follows. In Section 2 we derive an improved upper bound on the CP asymmetry ε_1 and illustrate how it can be saturated for specific neutrino mass matrices. Theoretical expectations for the range of neutrino masses are discussed in Section 3. In Section 4 we then derive upper bounds on the light neutrino masses in the cases of normal and inverted hierarchy, and we discuss the stability of these bounds. Section 5 deals with the washout of a large initial $B - L$ asymmetry, and a summary of our results is given in Section 6.

2 Bounds on the CP asymmetry

Given the masses of heavy and light Majorana neutrinos the CP asymmetry ε_1 in the decays of N_1, the lightest of the heavy neutrinos, satisfies an upper bound [10, 11]. In the following we shall study under which conditions this upper bound is saturated and how it depends on the effective neutrino mass $\widetilde{m}_1$ which plays an important role in the thermodynamic process of leptogenesis.

The standard model with right-handed neutrinos is described by the lagrangian,

$$\mathcal{L}_m = h_{ij}\bar{l}_{Li}\nu_{Rj}\phi + \frac{1}{2}M_{ij}\overline{\nu}^c_{Ri}\nu_{Rj} + h.c. \, , \tag{3}$$

where M is the Majorana mass matrix of the right-handed neutrinos, and the Yukawa couplings h yield the Dirac neutrino mass matrix $m_D = hv$ after spontaneous symmetry breaking, $v = \langle\phi\rangle$. We work in the mass eigenstate basis of the right-handed neutrinos where M is diagonal with real and positive eigenvalues $M_1 \leq M_2 \leq M_3$. The seesaw mechanism [6] then yields the light neutrino mass matrix

$$m_\nu = -m_D\frac{1}{M}m_D^T \, , \tag{4}$$

which can be diagonalized by a unitary matrix $U^{(\nu)}$,

$$U^{(\nu)\dagger}m_\nu U^{(\nu)*} = -\begin{pmatrix} m_1 & 0 & 0 \\ 0 & m_2 & 0 \\ 0 & 0 & m_3 \end{pmatrix} \, , \tag{5}$$

with real and positive eigenvalues satisfying $m_1 \leq m_2 \leq m_3$.

It is convenient to work in a basis where also the light neutrino mass matrix is diagonal. In this basis the Yukawa couplings are

$$\tilde{h} = U^{(\nu)\dagger}h \, . \tag{6}$$

As a consequence of the seesaw formula the matrix Ω,

$$\Omega_{ij} = \frac{v}{\sqrt{m_iM_j}}\tilde{h}_{ij} \, , \tag{7}$$

is orthogonal, $\Omega\Omega^T = \Omega^T\Omega = I$ [13]. It is then easy to show that the CP asymmetry ε_1 [14]-[16] is given by (cf., e.g., [9])

$$\varepsilon_1 = \frac{3}{16\pi}\frac{M_1}{v^2}\sum_{i\neq 1}\frac{\Delta m_{i1}^2}{m_i}\frac{\text{Im}\left(\tilde{h}_{i1}^2\right)}{\left(\tilde{h}^\dagger\tilde{h}\right)_{11}} \, , \tag{8}$$

where $\Delta m_{i1}^2 = m_i^2 - m_1^2$.

The CP asymmetry ε_1 is bounded by the maximal asymmetry ε_1^{max} [12],

$$|\varepsilon_1| \leq \varepsilon_1^{max} = \frac{3}{16\pi} \frac{M_1}{v^2} \frac{(\Delta m_{atm}^2 + \Delta m_{sol}^2)}{m_3} \ . \tag{9}$$

As we will now show, this bound holds for arbitrary values of m_2, i.e. for normal and for inverted hierarchy, and it is saturated in the limit $m_1 \to 0$.

Consider the normalized Yukawa couplings

$$z_i = \frac{\tilde{h}_{i1}^2}{(\tilde{h}^\dagger \tilde{h})_{11}} = x_i + i y_i \ , \tag{10}$$

with

$$0 \leq |z_i| \leq 1 \ , \quad \sum_i |z_i| = 1 \ . \tag{11}$$

The orthogonality condition $(\Omega^T \Omega)_{11} = 1$ yields the additional constraint

$$\sum_i \frac{\widetilde{m}_1}{m_i} z_i = 1 \ . \tag{12}$$

In the new variables the CP asymmetry reads

$$\varepsilon_1 = \frac{3}{16\pi} \frac{M_1}{v^2} \left(\frac{\Delta m_{21}^2}{m_2} y_2 + \frac{\Delta m_{31}^2}{m_3} y_3 \right) \ . \tag{13}$$

Since $m_3 > m_2$, one also has $\Delta m_{31}^2/m_3 > \Delta m_{21}^2/m_2$. This suggests that the maximal CP asymmetry is reached for maximal y_3.

Suppose now that $1 - y_3 = \mathcal{O}(\epsilon)$. Because of Eqs. (11) this implies y_2, y_1 and all x_i have to vanish in the limit $\epsilon \to 0$. The orthogonality condition $(\Omega^T \Omega)_{11} = 1$ yields

$$\frac{y_1}{m_1} + \frac{y_2}{m_2} + \frac{y_3}{m_3} = 0 \ , \tag{14}$$

$$\frac{\widetilde{m}_1}{m_1} x_1 + \frac{\widetilde{m}_1}{m_2} x_2 + \frac{\widetilde{m}_1}{m_3} x_3 = 1 \ . \tag{15}$$

Since $m_2 > 0$, these conditions are satisfied for maximal y_3, if $y_2 = x_2 = x_3 = 0$ and

$$m_1 \ , \ y_1 \propto \epsilon \ , \tag{16}$$

$$\widetilde{m}_1 \propto \epsilon^a \ , \quad x_1 \propto \epsilon^{1-a} \ , \quad 0 \leq a < 1 \ . \tag{17}$$

Note that in the limit $\epsilon \to 0$, N_1 couples only to $l_3\phi$. For $a > 0$, N_1 decouples completely, since $\tilde{h}_{i1}^2 = (\tilde{h}^\dagger \tilde{h})_{11} z_i$ and $(\tilde{h}^\dagger \tilde{h})_{11} \propto \widetilde{m}_1$.

An explicit example, which illustrates this saturation of the CP bound, is given by the following orthogonal matrix,

$$\Omega = \begin{pmatrix} A & 0 & -B \\ 0 & 1 & 0 \\ B & 0 & A \end{pmatrix} , \tag{18}$$

with

$$B^2 = i\frac{v^2}{m_3 M_1}b\epsilon^a , \quad A^2 = 1 - B^2 , \quad b > 0 . \tag{19}$$

The corresponding Yukawa couplings squared are

$$\left(\tilde{h}_{i1}^2\right) = \left(\frac{m_1 M_1}{v^2} - i\frac{m_1}{m_3}b\epsilon^a, 0, ib\epsilon^a\right) . \tag{20}$$

One obviously has $x_2 = x_3 = y_2 = 0$, and $y_3 \to 1$, $x_1, y_1 \to 0$ in the limit $\epsilon \to 0$. The matrix of Yukawa couplings,

$$\tilde{h} = \begin{pmatrix} \sqrt{\frac{m_1 M_1}{v^2} - i\frac{m_1}{m_3}b\epsilon^a} & 0 & \sqrt{i\frac{m_1 M_3}{m_3 M_1}b\epsilon^a} \\ 0 & \frac{\sqrt{m_2 M_2}}{v} & 0 \\ -\sqrt{ib\epsilon^a} & 0 & \sqrt{\frac{m_3 M_3}{v^2} - i\frac{M_3}{M_1}b\epsilon^a} \end{pmatrix} , \tag{21}$$

becomes diagonal in the limit $\epsilon \to 0$ for $a > 0$. Hence, in this basis, the large neutrino mixings are due to the charged lepton mass matrix.

This example illustrates that $\widetilde{m}_1$ can be arbitrary in the limit $m_1 \to 0$. It approaches $b^2 v^2/M_1$ for $a = 0$, while it goes to 0 for $a > 0$. Hence, the maximal CP asymmetry (9) can be reached for arbitrary values of m_2 and $\widetilde{m}_1$. For a given CP asymmetry, the maximal baryon asymmetry is reached in the limit $\widetilde{m}_1 \to 0$, assuming thermal initial N_1 abundance. The corresponding, model independent lower bound on the heavy neutrino mass M_1 was determined in [9] to be $M_1 > 4 \times 10^8$ GeV. If the Yukawa couplings $\tilde{h}$ are restricted, a more stringent lower bound on M_1 can be derived [17].

The above discussion can easily be extended to derive the maximal CP asymmetry in the case of arbitrary $\widetilde{m}_1$. Since $m_3 > m_2 > m_1$, one again has $x_3 = x_2 = y_2 = 0$. From Eqs. (14),(15) one then concludes

$$y_1 = -\frac{m_1}{m_3}y_3 , \quad x_1 = \frac{m_1}{\widetilde{m}_1} . \tag{22}$$

Together with the constraint (cf. (11)), $\sqrt{x_1^2 + y_1^2} + |y_3| = 1$, these conditions determine $|y_3|$ as function of m_1, m_3 and $\widetilde{m}_1$. Inserting the result into Eq. (13) yields the improved upper bound

$$\varepsilon_1^{max} = \frac{3}{16\pi}\frac{M_1 m_3}{v^2}\left[1 - \frac{m_1}{m_3}\left(1 + \frac{m_3^2 - m_1^2}{\widetilde{m}_1^2}\right)^{1/2}\right] . \tag{23}$$

6

For $m_1 = 0$ the result coincides with the previous bound (9). For $0 < m_1 \leq \widetilde{m}_1$ the new bound is more stringent. In particular, $\varepsilon_1^{max} = 0$ for $\widetilde{m}_1 = m_1$. Note that according to Eq. (23) the only model independent restriction on the effective neutrino mass is $\widetilde{m}_1 \geq m_1$. The improved upper bound on the CP asymmetry implies also a bound on the light neutrino masses which is more stringent than the one obtained in [12]. This will be discussed in Section 4.

3 Range of neutrino masses

At present we know two mass squared differences for the light neutrinos, which are deduced from the measurements of solar and atmospheric neutrino fluxes. In addition we have information about elements of the mixing matrix U in the leptonic charged current. Since U could be entirely due to mixings of the charged leptons, this does not constrain the light neutrino mass matrix in a model independent way. The light neutrino masses $m_1 < m_2 < m_3$ can be either quasi-degenerate or hierarchical, with $m_2 - m_1 \ll m_3 - m_2$ ('normal hierarchy') or $m_3 - m_2 \ll m_2 - m_1$ ('inverted hierarchy'). The best information on the absolute neutrino mass scale comes from neutrinoless double β-decay, which yields an upper bound on the light Majorana neutrino masses of about 1 eV [18, 19].

A crucial quantity for thermal leptogenesis is the effective neutrino mass $\widetilde{m}_1$ which is always larger than m_1 [20], as one easily sees from the orthogonality of Ω (cf. (7)),

$$
\begin{aligned}
\widetilde{m}_1 &= \frac{v^2}{M_1} \sum_i |\tilde{h}_{i1}^2| = \sum_i m_i |\Omega_{i1}^2| \\
&\geq m_1 \sum_i |\Omega_{i1}^2| \geq m_1 \sum_i \mathrm{Re}(\Omega_{i1}^2) = m_1 \, .
\end{aligned}
\tag{24}
$$

As we saw in the previous Section, the maximal CP asymmetry is reached for $m_1 = 0$, such that $m_2 \simeq \sqrt{\Delta m_{\mathrm{sol}}^2}$ and $m_3 \simeq \sqrt{\Delta m_{\mathrm{atm}}^2}$.

There is no model independent upper bound on $\widetilde{m}_1$. However, if there are no strong cancelations due to phase relations between different matrix elements, one has

$$
\widetilde{m}_1 \leq m_3 \sum_i |\Omega_{i1}^2| \sim m_3 |\sum_i \Omega_{i1}^2| = m_3 \, .
\tag{25}
$$

Hence, the natural range for the effective neutrino mass is $m_1 \leq \widetilde{m}_1 \lesssim m_3$. In fact, we are not aware of any neutrino mass model where this is not the case.

It is instructive to examine the range of $\widetilde{m}_1$ also in the special case $|\varepsilon_1| = \varepsilon_1^{\mathrm{max}}$. As we saw in the previous section this case is realized for $y_2 = x_2 = x_3 = 0$, corresponding to

$\mathrm{Re}(\Omega_{21}^2) = \mathrm{Re}(\Omega_{31}^2) = \mathrm{Im}(\Omega_{21}^2) = 0$. The orthogonality condition then implies $\mathrm{Im}(\Omega_{11}^2) = -\mathrm{Im}(\Omega_{31}^2)$ and $\mathrm{Re}(\Omega_{11}^2) = 1$. Hence, for maximal CP asymmetry one has

$$\widetilde{m}_1 = m_1 \sqrt{1 + \mathrm{Im}(\Omega_{31}^2)^2} + m_3 \left| \mathrm{Im}(\Omega_{31}^2) \right| , \qquad (26)$$

showing that the value of $\widetilde{m}_1$ is tuned by just one quantity. For $\mathrm{Im}(\Omega_{31}^2) = 0$, one has $\widetilde{m}_1 = m_1$, while the case $\widetilde{m}_1 \gg m_3$ corresponds to a fine tuned situation in which $|\mathrm{Im}(\Omega_{31}^2)| = |\mathrm{Im}(\Omega_{11}^2)| \gg \mathrm{Re}(\Omega_{11}^2) = 1$.

If the observed large mixing angles in the leptonic charged current originate from the neutrino mass matrix, which appears natural since their Majorana nature distinguishes neutrinos from quarks, the masses m_1 and $\widetilde{m}_1$ are related to m_2 and m_3. The seesaw mechanism together with leptogenesis then also constrains the heavy Majorana neutrino masses.

Large mixing angles are naturally explained if neutrino masses are quasi-degenerate [23]. One then has $\widetilde{m}_1 \approx m_1 \approx m_2 \approx m_3 > 0.1$ eV. However, as shown in [9, 12] and further strengthened in the following Section, quasi-degenerate neutrinos are strongly disfavored by thermal leptogenesis. A possible exception is the case where also the heavy Majorana neutrinos are partially degenerate. One then gets an enhancement of the CP asymmetry which allows one to increase the neutrino masses and still have successful leptogenesis. Models with $\Delta M_{21}/M_1 = (M_2 - M_1)/M_1 < 5 \times 10^{-2}$ and $\Delta M_{21}/M_1 = 5 \times 10^{-7}$ have been considered in refs. [25] and [26], respectively. Note, however, that in these examples the light neutrino masses are not quasi-degenerate. We shall pursue this case further in Section 4.3.

The neutrino mass pattern with inverted hierarchy has also received much attention in the literature. There is, however, the well known difficulty of this scenario to fit the large angle MSW solution [27, 28]. We also do not know any model with inverted hierarchy which incorporates successfully leptogenesis, and we shall therefore not pursue this case further.

We are then left with the case of neutrino masses with normal hierarchy. There are many neutrino mass models of this type with successful leptogenesis. The mass hierarchy is usually controlled by a parameter $\epsilon \ll 1$. For the effective neutrino mass one can then have, for instance, $\widetilde{m}_1 \sim m_2$ (cf. [26, 29]). A simple and attractive form of the light neutrino mass matrix, which can account for all data, is given by [30, 31],

$$m_\nu \sim \begin{pmatrix} \epsilon^2 & \epsilon & \epsilon \\ \epsilon & 1 & 1 \\ \epsilon & 1 & 1 \end{pmatrix} \frac{v^2}{M_3} , \qquad (27)$$

8

where coefficients $\mathcal{O}(1)$ have been omitted. This form could follow from a U(1) family symmetry [32] or a relation between the hierarchies of Dirac and Majorana neutrino masses [33]. In the second case one has $m_1, m_2 \sim \epsilon m_3$ and $\widetilde{m}_1 \sim m_3$, which is compatible with leptogenesis. The structure of the mass matrix (27) as well as predictions for the coefficients $\mathcal{O}(1)$ can be obtained in seesaw models where the exchange of two heavy Majorana neutrinos dominates [34]. In all these examples the range of the effective neutrino mass is $m_1 \leq \widetilde{m}_1 \lesssim m_3$.

Thermal leptogenesis also leads to a lower bound on M_1, the smallest of the heavy neutrino masses [35, 11]. In the minimal scenario, where the heavy neutrinos are not degenerate, one obtains the lower bound $M_1 > 4 \times 10^8$ GeV [9]. It is reached for maximal CP asymmetry ($m_1 = 0$), minimal washout ($\widetilde{m}_1 \rightarrow 0$), and assuming thermal initial N_1 abundance. The bound becomes more stringent for restricted patterns of mass matrices [17]. It can be relaxed if the heavy neutrinos are partially degenerate [24, 25, 26].

4 Improved upper bounds on neutrino masses

4.1 Maximal asymmetry and CMB constraint

It is useful to recast the maximal CP asymmetry (23) in the following way,

$$\varepsilon_1^{\max}(M_1, \widetilde{m}_1, \overline{m}) = 10^{-6} \left(\frac{M_1}{10^{10} \text{GeV}} \right) \frac{m_{\text{atm}}}{m_0} \, \beta(\widetilde{m}_1, \overline{m}) \, , \tag{28}$$

where $m_{\text{atm}} = \sqrt{\Delta m_{\text{atm}}^2 + \Delta m_{\text{sol}}^2}$, $m_0 = (16\,\pi/3)\,(v^2/10^{10} \text{ GeV}) \simeq 0.051$ eV, and

$$\beta(\widetilde{m}_1, \overline{m}) = \frac{\left(m_3 - m_1 \sqrt{1 + \frac{m_{\text{atm}}^2}{\widetilde{m}_1^2}} \right)}{m_{\text{atm}}} \leq 1 \quad . \tag{29}$$

The maximal value, $\beta = 1$, is obtained for $m_1 = 0$. Note, that $m_{\text{atm}} = m_0$ for the best fit values extracted from the KamLAND data [22], $\Delta m_{\text{sol}}^2 = 6.9 \times 10^{-5}$ eV², and the SuperKamiokande data [21], $\Delta m_{\text{atm}}^2 = 2.5 \times 10^{-3}$ eV².

We will calculate particle numbers and asymmetries normalized to the number of photons per comoving volume before the onset of leptogenesis at $t_\star$ [9]. For zero initial $B - L$ asymmetry, i.e. $N_{B-L}^{\text{i}} = 0$, the final $B - L$ asymmetry produced by leptogenesis is given by

$$N_{B-L}^{\text{f}} = -\frac{3}{4} \, \varepsilon_1 \, \kappa_{\text{f}} \, , \tag{30}$$

where κ_{f} is the 'efficiency factor'. In the minimal version of thermal leptogenesis one considers initial temperatures $T_i \gtrsim M_1$, where M_1 is the mass of the lightest heavy

9

neutrino N_1. In this case $\kappa_{\mathrm{f}} \leq 1$, and the maximal value, $\kappa_{\mathrm{f}} = 1$, is obtained for thermal initial N_1 abundance in the limit $\widetilde{m}_1 \to 0$. The heavy neutrinos N_1 then decay fully out of equilibrium at temperatures well below M_1, producing a $B - L$ asymmetry which survives until today since all washout processes are frozen at temperatures $T \ll M_1$.

In the case of general initial conditions and arbitrary values of $\widetilde{m}_1$, the efficiency factor κ_{f} has to be calculated by solving the Boltzmann equations [36, 37, 38, 39, 9],

$$\frac{dN_{N_1}}{dz} = -(D + S)(N_{N_1} - N_{N_1}^{\mathrm{eq}}) , \qquad (31)$$

$$\frac{dN_{B-L}}{dz} = -\varepsilon_1 D (N_{N_1} - N_{N_1}^{\mathrm{eq}}) - W N_{B-L} , \qquad (32)$$

where $z = M_1/T$. There are four classes of processes which contribute to the different terms in the equations: decays, inverse decays, $\Delta L = 1$ scatterings and processes mediated by heavy neutrinos. The first three all modify the N_1 abundance. Denoting by H the Hubble parameter, $D = \Gamma_D/(H z)$ accounts for decays and inverse decays, while $S = \Gamma_S/(H z)$ represents the $\Delta L = 1$ scatterings. The decays are also the source term for the generation of the $B - L$ asymmetry, the first term in Eq. (32), while all the other processes contribute to the total washout term $W = \Gamma_W/(H z)$ which competes with the decay source term.

We take into account only decays of N_1, neglecting the decays of the heavier neutrinos N_2 and N_3. These decays produce a $B - L$ asymmetry at temperatures higher than M_1. As we shall see in Section 5, the washout processes at $T \sim M_1$ very efficiently erase any previously generated asymmetry. Even in the case of very small mass differences the decays of N_2 and N_3 do not change significantly the bound on the light neutrino masses, which is our main interest. This will be discussed in Section 4.3.

The baryon to photon number ratio at recombination, η_B, is simply related to N_{B-L}^{f} by $\eta_B = (a/f) N_{B-L}^{\mathrm{f}}$, where $a = 28/79$ [40] is the fraction of $B - L$ asymmetry which is converted into a baryon asymmetry by sphaleron processes, and $f = N_\gamma^{\mathrm{rec}}/N_\gamma^{\star} = 2387/86$ accounts for the dilution of the asymmetry due to standard photon production from the onset of leptogenesis till recombination. η_B^{max}, the final baryon asymmetry produced by leptogenesis with maximal CP asymmetry, i.e. $\varepsilon_1 = \varepsilon_1^{\mathrm{max}}$), is given by

$$\eta_B^{\mathrm{max}} \simeq 0.96 \times 10^{-2} \, \varepsilon_1^{\mathrm{max}} \, \kappa_{\mathrm{f}} . \qquad (33)$$

This quantity has to be compared with measurements of the CMB experiments BOOMerANG [41] and DASI [42],

$$\eta_B^{CMB} = (6.0_{-0.8}^{+1.1}) \times 10^{-10} . \qquad (34)$$

The CMB constraint then requires $\eta_B^{\max} \geq \eta_B^{CMB}$, and we will adopt for η_B^{CMB} the 3σ lower limit, $(\eta_B^{CMB})_{\text{low}} = 3.6 \times 10^{-10}$.

In [9] we showed that $\eta_B^{\max}$ depends just on the three parameters $\widetilde{m}_1, M_1$ and $\overline{m}$. Thus, for a given value of $\overline{m}$, the CMB constraint determines an allowed region in the $(\widetilde{m}_1, M_1)$-plane. It was also shown that there is an upper bound for $\overline{m}$ above which no allowed region exists. In [12], based on the bound (9) for the CP asymmetry, $\overline{m} < 0.30\,\text{eV}$ was derived as upper bound on the neutrino mass scale. In the following we shall study the allowed regions in the $(\widetilde{m}_1, M_1)$-plane for different parameters $\overline{m}$ using the improved bound on the CP asymmetry (23) and in this way determine a new improved bound on $\overline{m}$.

4.2   Numerical results

The neutrino masses m_1 and m_3 depend in a different way on $\overline{m}$ in the cases of normal and inverted hierarchy, respectively. Hence, also the dependence of the function β on $\overline{m}$ is different for these two mass patterns. This leads to different maximal baryon asymmetries $\eta_B^{\max}$, and therefore to different upper bounds on $\overline{m}$, in the two cases which we now study in turn.

For neutrino masses with normal hierarchy one has

$$m_3^2 - m_2^2 = \Delta m_{\text{atm}}^2\ , \quad m_2^2 - m_1^2 = \Delta m_{\text{sol}}^2\ , \tag{35}$$

and the dependence on $\overline{m}$ is given by

$$m_3^2 = \frac{1}{3}\left(\overline{m}^2 + 2\Delta m_{\text{atm}}^2 + \Delta m_{\text{sol}}^2\right)\ , \tag{36}$$

$$m_2^2 = \frac{1}{3}\left(\overline{m}^2 - \Delta m_{\text{atm}}^2 + \Delta m_{\text{sol}}^2\right)\ , \tag{37}$$

$$m_1^2 = \frac{1}{3}\left(\overline{m}^2 - \Delta m_{\text{atm}}^2 - 2\Delta m_{\text{sol}}^2\right)\ . \tag{38}$$

These relations are plotted in Fig. 1. Note that there is a minimal value of $\overline{m}$, corresponding to $m_1 = 0$, which is given by $\overline{m}_{\min} = \sqrt{\Delta m_{\text{atm}}^2 + 2\Delta m_{\text{sol}}^2} \simeq 0.051\,\text{eV}$.

Fig. 2 shows the lines of constant maximal baryon asymmetry $\eta_B^{\max} = (\eta_B^{CMB})_{\text{low}}$ (thick lines) and $\eta_B^{\max} = 10^{-10}$ (thin lines) in the $(\widetilde{m}_1, M_1)$-plane for different choices of $\overline{m}$ and assuming zero initial N_1 abundance. The allowed regions (the filled ones) correspond to the constraint $\eta_B^{\max} \geq (\eta_B^{CMB})_{\text{low}}$. The largest allowed region is obtained for $\overline{m} = \overline{m}_{\min}$, since in this case the CP asymmetry is maximal, i.e. $\beta = 1$ for any value of $\widetilde{m}_1$, and the washout is minimal. Note that a different choice for the initial N_1 abundance would have affected the final baryon asymmetry only for $\widetilde{m}_1 < m_*$. The case of an initial thermal
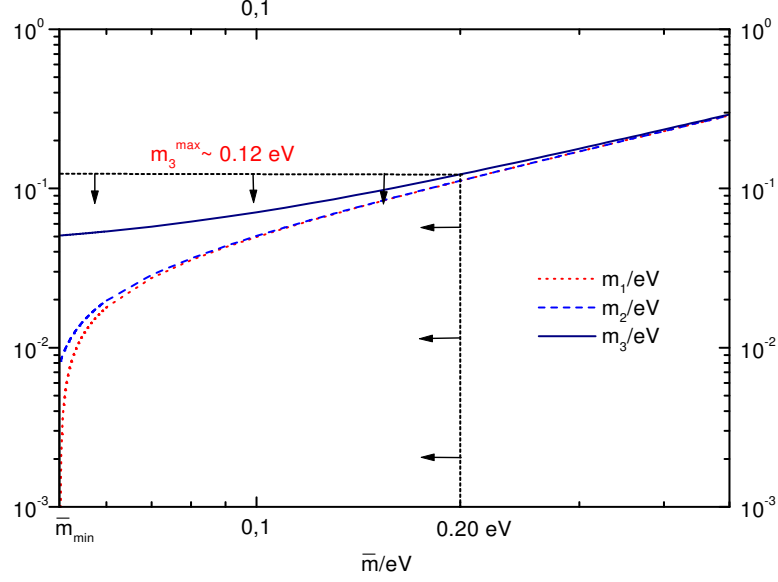
11

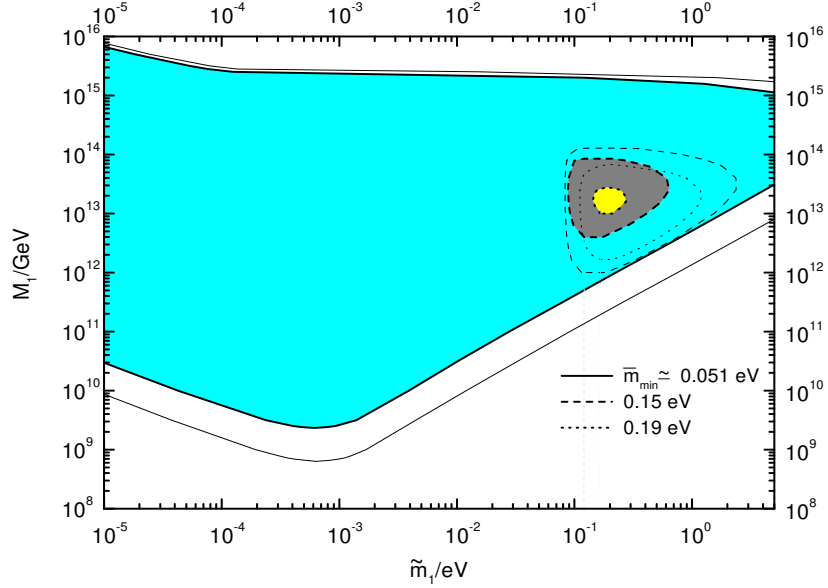Figure 1: Neutrino masses as functions of $\overline{m}$ for normal hierarchy (cf. (36)-(38)).

Figure 2: Normal hierarchy case. Curves, in the $(\widetilde{m}_1\text{-}M_1)$-plane, of constant $\eta_{B0}^{\max} = 10^{-10}$ (thin lines) and $\eta_{B0}^{\max} = 3.6 \times 10^{-10}$ (thick lines) for the indicated values of $\overline{m}$. The filled regions for $\eta_{B0}^{\max} \geq 3.6 \times 10^{-10}$ are the *allowed regions* from CMB. There is no allowed region for $\overline{m} = 0.20\,\mathrm{eV}$.

abundance has been studied in [9]. When $\overline{m}$ increases different effects combine to shrink the allowed region until it completely disappears at some value $\overline{m}_{\text{max}}$.

We have determined this value with a numerical uncertainly of $0.01\,\text{eV}$. From Fig. 2 one can see that there is a small allowed region for $\overline{m} = 0.19\,\text{eV}$, whereas we found no allowed region for $\overline{m} = 0.20\,\text{eV}$. Hence, the value of $\overline{m}_{\text{max}}$ is somewhere in between and we can conclude that in the case of normal hierarchy,

$$\overline{m} < 0.20\,\text{eV} \ . \tag{39}$$

Using the relations (36)-(38), one can easily translate this bound into upper limits on the individual neutrino masses (cf. Fig. 1),

$$m_1, m_2 < 0.11\,\text{eV} \ , \quad m_3 < 0.12\,\text{eV} \ . \tag{40}$$

The case of an inverted hierarchy of neutrino masses corresponds to

$$m_3^2 - m_2^2 = \Delta m_{\text{sol}}^2 \ , \quad m_2^2 - m_1^2 = \Delta m_{\text{atm}}^2 \ , \tag{41}$$

and the relations between the neutrino masses and $\overline{m}$ are

$$m_3^2 \ = \ \frac{1}{3} \left(\overline{m}^2 + \Delta m_{\text{atm}}^2 + 2\,\Delta m_{\text{sol}}^2 \right) \ , \tag{42}$$

$$m_2^2 \ = \ \frac{1}{3} \left(\overline{m}^2 + \Delta m_{\text{atm}}^2 - \Delta m_{\text{sol}}^2 \right) \ , \tag{43}$$

$$m_1^2 \ = \ \frac{1}{3} \left(\overline{m}^2 - 2\,\Delta m_{\text{atm}}^2 - \Delta m_{\text{sol}}^2 \right) \ . \tag{44}$$

We have plotted these relations in Fig. 3. The minimal value of $\overline{m}$, corresponding to $m_1 = 0$, is now $\overline{m}_{\text{min}} = \sqrt{2\,\Delta m_{\text{atm}}^2 + \Delta m_{\text{sol}}^2} \simeq 0.072\,\text{eV}$.

The curves of constant η_B^{max} are shown in Fig. 4 for different values of $\overline{m}$. The largest allowed region is again obtained for $\overline{m} = \overline{m}_{\text{min}}$. One can see that this time there is a tiny allowed region for $\overline{m} = 0.20\,\text{eV}$ and no allowed region for $\overline{m} = 0.21\,\text{eV}$. Therefore, in the case of inverted hierarchy the upper bound is slightly relaxed,

$$\overline{m} < 0.21\,\text{eV} \ . \tag{45}$$

Using the relations (42)-(44) one can again translate the bound on $\overline{m}$ into bounds on the individual neutrino masses,

$$m_1 < 0.11\,\text{eV} \ , \quad m_2, m_3 < 0.12\,\text{eV} \ . \tag{46}$$

Let us now discuss the different effects which combine to shrink the allowed region when the absolute neutrino mass scale $\overline{m}$ increases, thus yielding the upper bound. The
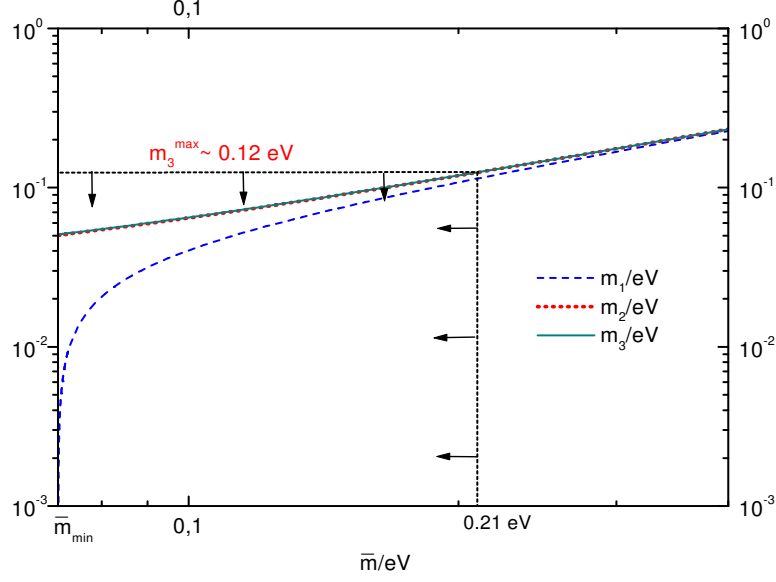
13

Figure 3: Neutrino masses as functions of $\overline{m}$ for inverted hierarchy (cf. (42)-(44)).
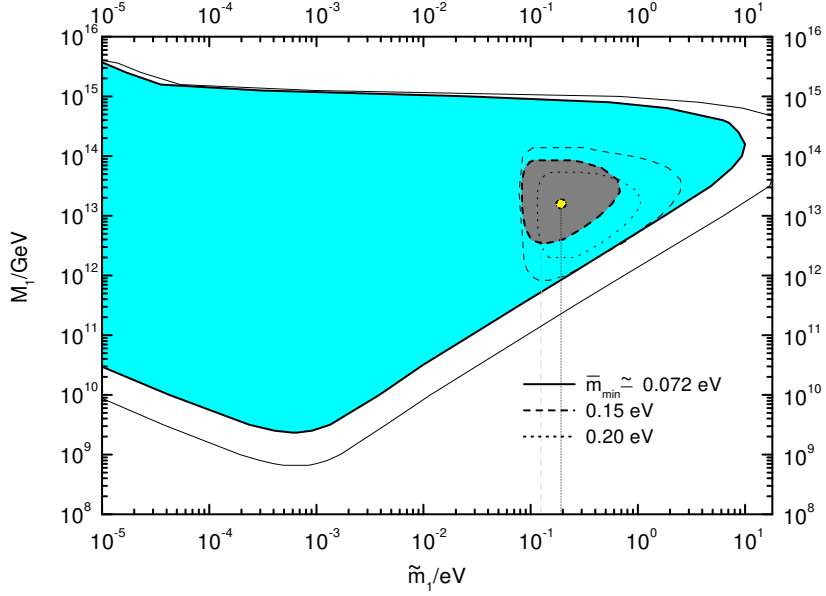

Figure 4: Inverted hierarchy case. Curves, in the $(\widetilde{m}_1\text{-}M_1)$-plane, of constant $\eta_{B0}^{\max} = 10^{-10}$ (thin lines) and $\eta_{B0}^{\max} = 3.6 \times 10^{-10}$ (thick lines) for the indicated values of $\overline{m}$. The filled regions for $\eta_{B0}^{\max} \geq 3.6 \times 10^{-10}$ are the *allowed regions* from CMB. There is no allowed region for $\overline{m} = 0.20$ eV.
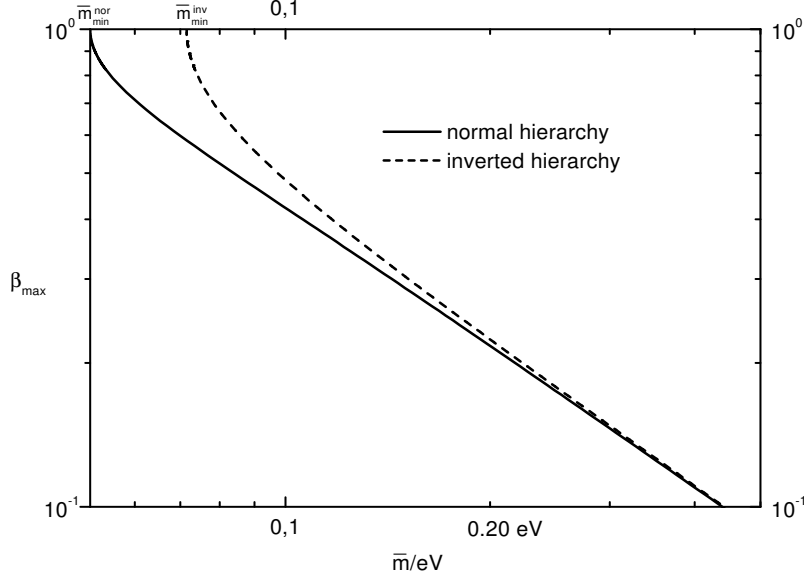
Figure 5: The CP asymmetry global suppression factor β_{max} for normal and inverted hierarchy.

first effect is that away from the hierarchical neutrino case, for $\overline{m} > \overline{m}_{\mathrm{min}}$ and $m_1 > 0$, the maximal CP asymmetry reduces considerably. This can be seen in terms of the function β (cf. (29)) which is conveniently expressed in the form

$$\beta = \beta_{\mathrm{max}}(\overline{m}) \, f(\widetilde{m}_1, \overline{m}) \; . \tag{47}$$

The first factor, $\beta_{\mathrm{max}} = (m_3 - m_1)/m_{\mathrm{atm}} = m_{\mathrm{atm}}/(m_3 + m_1)$, is the maximal value of β for fixed $\overline{m}$; β_{max} decreases $\propto 1/\overline{m}$ for $\overline{m} \gg \overline{m}_{\mathrm{min}}$ (cf. Fig. 5). This implies that for increasing $\overline{m}$ there is an overall suppression of the maximal baryon asymmetry in the whole $(\widetilde{m}_1, M_1)$-plane [11]. In particular the lower limit on M_1 becomes more stringent.

The factor $f(\widetilde{m}_1, \overline{m}) = 1$, for any value of $\widetilde{m}_1$, if $\overline{m} = \overline{m}_{\mathrm{min}}$ $(m_1 = 0)$. In the case $\overline{m} > \overline{m}_{\mathrm{min}}$ $(m_1 > 0)$ it vanishes for $\widetilde{m}_1 = m_1$ and grows monotonically to 1 with increasing $\widetilde{m}_1$ (cf. Fig. 6). Thus for $m_1 > 0$ the function f gives a further suppression of the CP asymmetry, in addition to the one from $\beta_{\mathrm{max}} < 1$. This suppression is strong for $\widetilde{m}_1 \gtrsim m_1$ and disappears for $\widetilde{m}_1 \gg m_1$. Hence the decrease of the maximal CP asymmetry for $\overline{m} > \overline{m}_{\mathrm{min}}$ shrinks the allowed region most at small $\widetilde{m}_1 \gtrsim m_1$ and at small M_1. Note that the difference between the allowed regions for normal and inverted hierarchy is accounted for by the different values of β for a given value of $\overline{m}$. In the case of inverted hierarchy β is larger for any value of $\widetilde{m}_1$ and $\overline{m} \geq \overline{m}_{\mathrm{min}}^{\mathrm{inv}}$ (cf. Figs. 5,6). The effect is maximal for $\overline{m} = \overline{m}_{\mathrm{min}}^{\mathrm{inv}}$ where $\beta^{\mathrm{inv}} = 1$ while $\beta^{\mathrm{nor}} \simeq 0.6$. For larger values of $\overline{m} \gg \overline{m}_{\mathrm{min}}^{\mathrm{inv}}$, and also
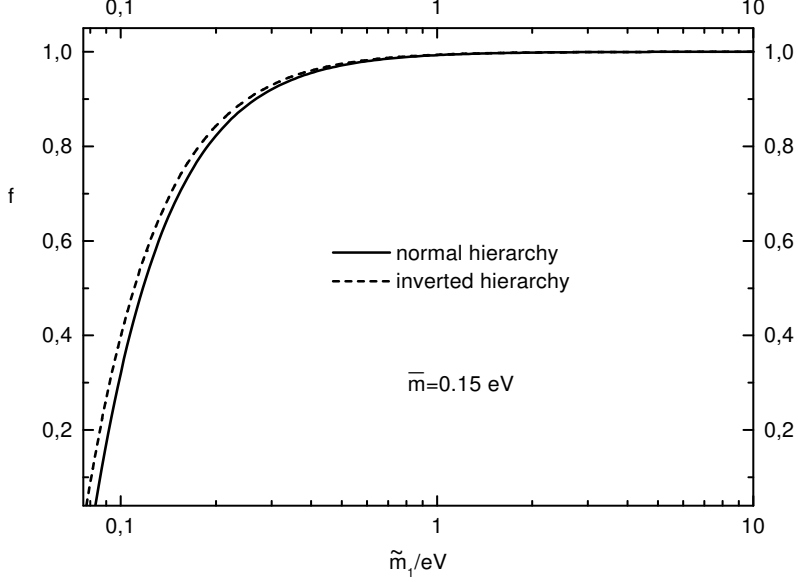
15

Figure 6: The function $f(\widetilde{m}_1, \overline{m} = 0.15\,\text{eV})$ for normal (inverted) hierarchy. It is defined for $\widetilde{m}_1 \geq m_1 \simeq 0.08\,(0.07)\,\text{eV}$.

$\widetilde{m}_1 \gg m_1^{\text{nor}}$, the ratio $\beta^{\text{inv}}/\beta^{\text{nor}}$ becomes very close to 1. This situation is realized when $\overline{m}$ approaches its upper bound. This explains why the upper bound on $\overline{m}$ is only slightly relaxed in the case of inverted hierarchy.

The second effect, which shrinks the allowed region when $\overline{m}$ increases, is the enhancement of washout processes. In [9] we showed how the total washout rate can be written as the sum of two terms, $(W - \Delta W) \propto \widetilde{m}_1$ and $\Delta W \propto M_1\,\overline{m}^2$. The first term is responsible for the reduction of the allowed region at large $\widetilde{m}_1$. The second term leads to the boundary at large M_1. The combined effect shrinks the allowed region with increasing $\overline{m}$ at large M_1 and at large $\widetilde{m}_1$.

One can see how this second effect reduces the allowed region, independent of the maximal CP asymmetry decrease, by comparing the two largest allowed regions for normal and inverted hierarchy; they correspond to the two different values of $\overline{m}_{\text{min}}$ (cf. Fig. 2 and Fig. 4). Since $\beta = 1$ in both cases, the entire difference is due to the different washout effects. They are larger in the case of inverted hierarchy because $\overline{m}_{\text{min}}$ is about $\sim \sqrt{2}$ higher than in the normal hierarchy case. One can see how, for a fixed value of $\widetilde{m}_1$, the maximal value of M_1 is approximately halved in the inverted hierarchy case. Correspondingly, the maximal allowed value of $\widetilde{m}_1$ is lower for inverted hierarchy than for normal hierarchy.

16

In summary, within the theoretical uncertainties, leptogenesis cannot distinguish between normal and inverted hierarchical neutrino mass patterns. However, our new analysis confirms and strengthens the results of [9, 12] that quasi-degenerate neutrino masses are strongly disfavored by leptogenesis, by putting the stringent upper bound of 0.12 eV on all neutrino masses.

4.3   Stability of the bound

The numerical results can be very well reproduced analytically [43]. This procedure is not only able to yield the correct value of $\overline{m}_{\mathrm{max}}$ but also reveals some general features which in the numerical analysis may appear accidental.

For $\overline{m} = \overline{m}_{\mathrm{max}}$, at the peak value of maximal asymmetry, such that $\eta_B^{\mathrm{max}} = \eta_B^{CMB}$, one has

$$\widetilde{m}_1|_{\mathrm{max}} = \overline{m}_{\mathrm{max}} + \mathcal{O}\left(\frac{m_{\mathrm{atm}}^2}{\overline{m}_{\mathrm{max}}^2}\right) , \tag{48}$$

$$M_1|_{\mathrm{max}} \simeq 1.6 \times 10^{13}\,\mathrm{GeV}\,\left(\frac{0.2\,\mathrm{eV}}{\overline{m}_{\mathrm{max}}}\right)^2 . \tag{49}$$

The value of $\overline{m}_{\mathrm{max}}$ is slightly different for normal and inverted hierarchy, respectively,

$$(\overline{m}_{\mathrm{max}}^{\mathrm{nor}})^2 = (\overline{m}_{\mathrm{max}}^0)^2 - \frac{1}{8}\,m_{\mathrm{atm}}^2 + \mathcal{O}(m_{\mathrm{atm}}^4/\overline{m}_{\mathrm{max}}^4) , \tag{50}$$

$$(\overline{m}_{\mathrm{max}}^{\mathrm{inv}})^2 = (\overline{m}_{\mathrm{max}}^0)^2 + \frac{7}{8}\,m_{\mathrm{atm}}^2 + \mathcal{O}(m_{\mathrm{atm}}^4/\overline{m}_{\mathrm{max}}^4) , \tag{51}$$

where $\overline{m}_{\mathrm{max}}^0$ is the zero-th order approximation. This implies

$$(\overline{m}_{\mathrm{max}}^{\mathrm{inv}})^2 - (\overline{m}_{\mathrm{max}}^{\mathrm{nor}})^2 = m_{\mathrm{atm}}^2 + \mathcal{O}(m_{\mathrm{atm}}^4/\overline{m}_{\mathrm{max}}^4) . \tag{52}$$

Besides gaining more insight into the numerical results, the analytic procedure also allows to find the dependence of the bound on the involved physical parameters and to study in this way its stability.

Consider first the dependence on the experimental quantities η_B^{CMB}, $\Delta m_{\mathrm{atm}}^2$ and $\Delta m_{\mathrm{sol}}^2$. Since $\Delta m_{\mathrm{sol}}^2 \ll \Delta m_{\mathrm{atm}}^2$, the dependence on $\Delta m_{\mathrm{sol}}^2$ is so small that it can be neglected, yielding $m_{\mathrm{atm}} \simeq \sqrt{\Delta m_{\mathrm{atm}}^2}$. The analytic procedure shows that $\overline{m}_{\mathrm{max}} \propto (m_{\mathrm{atm}}^2/\eta_B^{CMB})^{1/4}$. From the numerical result, found for $\eta_B^{CMB} = 3.6 \times 10^{-10}$ and $m_{\mathrm{atm}} = m_0 \simeq 0.051\,\mathrm{eV}$, and one then obtains in general

$$\overline{m}_{\mathrm{max}}^0 \simeq 0.175\,\mathrm{eV}\,\left(\frac{6 \times 10^{-10}}{\eta_B^{CMB}}\right)^{\frac{1}{4}}\,\left(\frac{m_{\mathrm{atm}}}{m_0}\right)^{\frac{1}{2}} . \tag{53}$$

Using Eq. (53) one immediately gets the central value of $\overline{m}_{\max}$. Note also that for $\eta_B^{CMB} = 10^{-10}$ and $m_{\text{atm}} = m_0$, one has $\overline{m}_{\max}^0 \simeq 0.275$ eV. This is confirmed by the numerical results. We still find iso-lines $\eta_B^{CMB} = 10^{-10}$ for $\overline{m} = 0.27$ eV, whereas this is not the case anymore for $\overline{m} = 0.28$ eV. From Eq. (53) one obtains as estimate for the relative error,

$$\delta \overline{m}_{\max} = \frac{1}{4} \left(\delta \eta_B^{CMB} + \delta m_{\text{atm}}^2 \right) \ . \tag{54}$$

According to Eq. (34) the 1σ standard error on η_B^{CMB} is about 15% while $\delta m_{\text{atm}}^2 \simeq 25\%$ [21]. We thus obtain $\delta \overline{m}_{\max} \simeq 10\%$, which corresponds to the absolute error $\Delta \overline{m}_{\max} \simeq 0.02$ eV. In the coming years the errors on η_B^{CMB} and m_{atm}^2 will be greatly reduced by the satellite experiments MAP [44] and Planck [45], and by the long baseline experiments Minos [46] and CNGS [47], respectively, and consequently the error on $\overline{m}_{\max}$ will be considerably reduced.

Another important question concerns the enhancement of the maximal CP asymmetry when $\Delta M_{21} = M_2 - M_1$, where M_1 and M_2 are the masses of the heavy neutrinos N_1 and N_2, becomes comparable to or smaller than M_1 itself. As long as the mass splitting is larger than the decay widths, the enhancement is given by [15, 16],

$$\xi(x) = \frac{2}{3} x \left[(1 + x) \ln \left(\frac{1 + x}{x} \right) - \frac{2 - x}{1 - x} \right] \ , \tag{55}$$

where $x = (M_2/M_1)^2$. Note, that ξ approaches 1 for $x \gg 1$. The value of $\overline{m}_{\max}$ increases like $\xi^{1/4}$ [43], and it is therefore easy to see how the bound on $\overline{m}$ gets relaxed for small values of the mass difference ΔM_{21}.

In Fig. 7 we have plotted the enhancement $\xi - 1$ and the central value of $\overline{m}_{\max}$, together with its 1σ limits, as function of $\Delta M_{21}/M_1$. For $\Delta M_{21}/M_1 \gtrsim 1$ the bounds (39),(45) are recovered. Only for values $\Delta M_{21}/M_1 \lesssim 0.1$ the bound gets relaxed in an appreciable way. An increase of $\overline{m}_{\max}$ by a factor ~ 3, allowing quasi-degenerate neutrino masses of 0.4 eV, which could be detected with the KATRIN experiment [48], requires degeneracies $\Delta M_{21}/M_1, \Delta M_{31}/M_1 \lesssim 10^{-3}$.

In the regime $\Delta M_{21} \lesssim M_1$ also decays of N_2 have to be taken into account. As we shall see in the next section, for larger mass splittings an asymmetry generated in N_2 decays would be washed out before $T \sim M_1$, and it is then sufficient to consider only N_1 decays. However, even for $\Delta M_{21}/M_1 \lesssim 0.1$, it is easy to see that the effect of such an additional asymmetry on the bound is small compared to the effect of the CP asymmetry enhancement described above. The largest effect would be obtained for $\varepsilon_2^{\max} = \varepsilon_1^{\max}$ and $\widetilde{m}_2 \ll \widetilde{m}_1$, corresponding to a doubled heavy neutrino abundance without any washout enhancement. In this extreme case the bound is relaxed at most by a factor $2^{1/4} \simeq 1.2$.
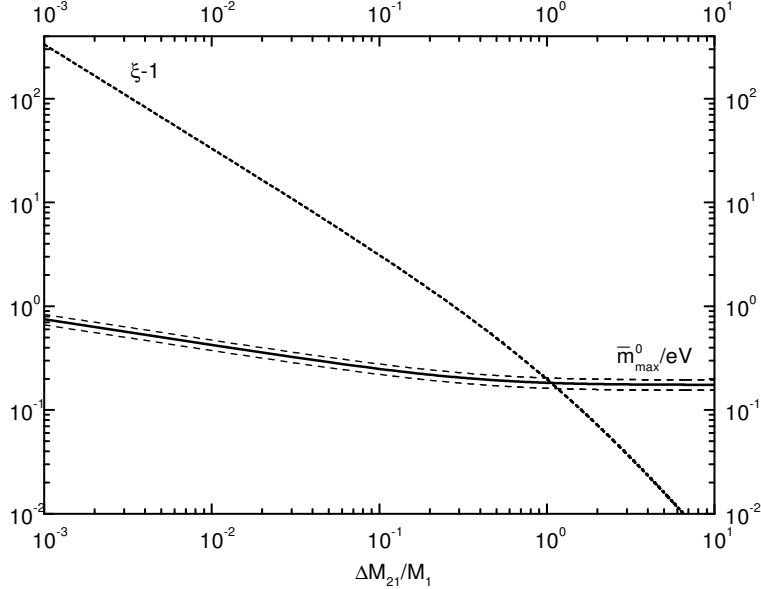
18

Figure 7: The CP asymmetry enhancement $\xi - 1$ (short dashed line) and $\langle \overline{m}^0_{\max} \rangle \pm \Delta \overline{m}^0_{\max}$ for normal hierarchy (solid and dashed lines) as functions $\Delta M_{21}/M_1$.

Even for three degenerate neutrinos, with both $\Delta M_{21}/M_1 \ll 1$ and $\Delta M_{31}/M_1 \ll 1$, the effect could relax the bound not more than by a factor $3^{1/4} \simeq 1.3$. Hence, the CP enhancement represents the dominant effect and we can conclude that the bound on $\overline{m}$ can only be evaded in case of an extreme degeneracy among the heavy Majorana neutrinos.

A further important issue is the effect of supersymmetry on the bound. In this case the maximal CP asymmetry is about twice as large which could relax the bound by a factor $2^{1/4} \sim 1.2$. However, washout processes are also considerably enhanced [38]. This effect goes into the opposite direction and is actually stronger, so that one can expect a slightly more stringent bound on $\overline{m}$. A detailed calculation will be presented in [43].

We conclude that the leptogenesis upper bound on neutrino masses is very stable. The essential reason is that, at $\overline{m} = \overline{m}_{\max}$, the peak value $\eta_B^{\max} \propto 1/\overline{m}_{\max}^4$. Hence, any variation of the final asymmetry results into change of $\overline{m}_{\max}$ which is almost one order of magnitude smaller. The same argument applies also to the theoretical uncertainties. Although the various corrections to the Boltzmann equations still remain to be calculated, we do not expect a relaxation of $\overline{m}_{\max}$ by more than 20%. In fact, we expect that the corrections will go in the direction of lowering the prediction on the final asymmetry, which will make the bound on $\overline{m}$ more stringent.

For particular patterns of neutrino mass matrices stronger bounds on the light neutrino

masses can be obtained. For instance, one can study how the upper bound changes if M_1 is required to be smaller than some cut-off value $M_1^\star$. For $M_1^\star > M_1|_{\max} \simeq 10^{13}\,\mathrm{GeV}$ (cf. (49)) the bound does not change. For smaller values of M_1 the bound becomes more stringent. For example, from Figs. 2 and 4 one can see that the cut-off $M_1 < 5 \times 10^{12}\,\mathrm{GeV}$ leads to the bound $\overline{m} < 0.15\,\mathrm{eV}$, which corresponds to $m_1 < 0.08\,\mathrm{eV}$. For a restricted mass pattern, and neglecting $\Delta W \propto M_1 \overline{m}^2$ washout terms, less stringent bounds have been found in [17] for the same cut-off value of M_1.

5   Dependence on initial conditions

A very important question for leptogenesis, and baryogenesis in general, is the dependence on initial conditions. This includes the dependence on the initial abundance of heavy Majorana neutrinos, which has been studied in detail in [9], and also the effect of an initial asymmetry which may have been generated by some other mechanism. In the following we shall study the efficiency of the washout of a large initial asymmetry by heavy Majorana neutrinos.

For simplicity, we neglect the small asymmetry generated through the CP violating interactions of the heavy neutrinos, i.e. we set $\varepsilon_1 = 0$. The kinetic equation (32) for the asymmetry then becomes

$$\frac{dN_{B-L}}{dz} = -W\,N_{B-L} \,, \tag{56}$$

where $-N_{B-L}$ is the number of lepton doublets per comoving volume. The final $B-L$ asymmetry is then given by

$$N_{B-L}^{\mathrm{f}} = \omega(z_{\mathrm{i}}) N_{B-L}^{\mathrm{i}} \,, \tag{57}$$

with the washout factor

$$\omega(z_{\mathrm{i}}) = e^{-\int_{z_{\mathrm{i}}}^{\infty} dz\, W(z)} \,. \tag{58}$$

In Eq. (56) $W(z) = \Gamma_W(z)/H(z)z$ is the rescaled washout rate, where $H(z)$ is the temperature-dependent Hubble parameter. Γ_W receives contributions from inverse decays (Γ_{ID}), $\Delta L = 1$ processes ($\Gamma_{\phi,t}$, $\Gamma_{\phi,s}$) and $\Delta L = 2$ processes (Γ_N, $\Gamma_{N,t}$) (cf. [9]),

$$\Gamma_W = \frac{1}{2}\Gamma_{ID} + 2\left(\Gamma_N^{(l)} + \Gamma_{N,t}^{(l)}\right) + 2\Gamma_{\phi,t}^{(l)} + \frac{n_{N_1}}{n_{N_1}^{\mathrm{eq}}}\Gamma_{\phi,s}^{(l)} \,. \tag{59}$$

The inverse decay rate is given by

$$\Gamma_{ID} = \frac{n_{N_1}^{\mathrm{eq}}}{n_l^{\mathrm{eq}}}\,\Gamma_D \,, \quad \Gamma_D = \frac{1}{8\pi}\left(h^\dagger h\right)_{11} M_1 \frac{K_1(z)}{K_2(z)} \,, \tag{60}$$

20

where $n_{N_1}^{\rm eq}$ and $n_l^{\rm eq}$ are the equilibrium number densities of heavy neutrinos and lepton doublets, respectively, and $K_{1,2}(z)$ are modified Bessel functions of the third kind. The quantities $\Gamma_i^{(X)}$ are thermally averaged reaction rates per particle X. They are related by $\Gamma_i^{(X)} = \gamma_i / n_X^{\rm eq}$ to the reaction densities γ_i [36]. Our calculations are based on the reduced cross sections given in ref. [38].

It is very instructive to consider analytical approximations to the various washout contributions. Both, the inverse decay rate and the resonance part of $\Gamma_N^{(l)}$ (cf. [9]) are proportional to $K_1(z)$,

$$\Gamma_W^{(1)} = \frac{1}{2}\Gamma_{ID} + 2\Gamma_{N,res}^{(l)} = \frac{1}{16\pi\zeta(3)}\left(h^\dagger h\right)_{11} M_1 z^2 K_1(z) \ . \tag{61}$$

The integral in Eq. (56) can be analytically performed. The corresponding washout factor can be written in the form

$$\omega^{(1)}(z_{\rm i}) = \exp\left\{-\frac{1}{2\zeta(3)}\frac{\widetilde{m}_1}{m_*}\left(\frac{3\pi}{2} + z_i^3 K_2(z_i) - \frac{3\pi}{2}z_i\left(K_2(z_i)L_1(z_i) + L_2(z_i)K_1(z_i)\right)\right)\right\},\tag{62}$$

where m_* is the equilibrium mass (2), and $L_{1,2}(z)$ are modified Struve functions [49]. Rather accurate approximations are, for small and large values of $z_{\rm i}$ respectively,

$$\omega^{(1)}(z_{\rm i}) = \begin{cases} \exp\left\{-\frac{1}{2\zeta(3)}\frac{\widetilde{m}_1}{m_*}\left(\frac{3\pi}{2} - \frac{1}{3}z_i^3 + \mathcal{O}(z_i^5)\right)\right\} \ , \ z_{\rm i} < 1 \\[2mm] \exp\left\{-\frac{1}{2\zeta(3)}\frac{\widetilde{m}_1}{m_*}\sqrt{\frac{\pi}{2z_i}}e^{-z_i}\left(z_i^3 + \frac{23}{8}z_i^2 + \frac{537}{128}z_i + \frac{2253}{1024} + \mathcal{O}(\frac{1}{z_i})\right)\right\} \ , \ z_i > 1 \ . \end{cases}\tag{63}$$

The non-resonant contribution of N_1 exchange to the washout is proportional to $\overline{m}^2$,

$$\begin{aligned} \Gamma_W^{(2)} &= 2\left(\Gamma_{N,nonres}^{(l)} + \Gamma_{N,t}^{(l)}\right) \\ &= \frac{1}{\pi^3\zeta(3)}\frac{M_1^3\overline{m}^2}{v^4}\frac{1}{z^3} \ , \end{aligned}\tag{64}$$

which yields the washout factor

$$\omega^{(2)}(z_{\rm i}) = \exp\left\{-\frac{8}{\pi^2\zeta(3)}\frac{M_1\overline{m}^2}{m_*v^2}\frac{1}{z_i}\right\} \ . \tag{65}$$

Finally, we have to consider N_1-top scatterings. The rate is dominated by t-channel Higgs exchange if the infrared divergence is cut off by a Higgs mass $m_\phi \sim 1$ TeV $\ll T$. In terms of the reduced cross section one has (cf. [38]),

$$\Gamma_{\phi,t}^{(l)} = \frac{M_1 z^2}{96\pi^2\zeta(3)}\int_1^\infty dx\sqrt{x}\hat{\sigma}_{\phi,t}(x)K_1(z\sqrt{x}) \ . \tag{66}$$
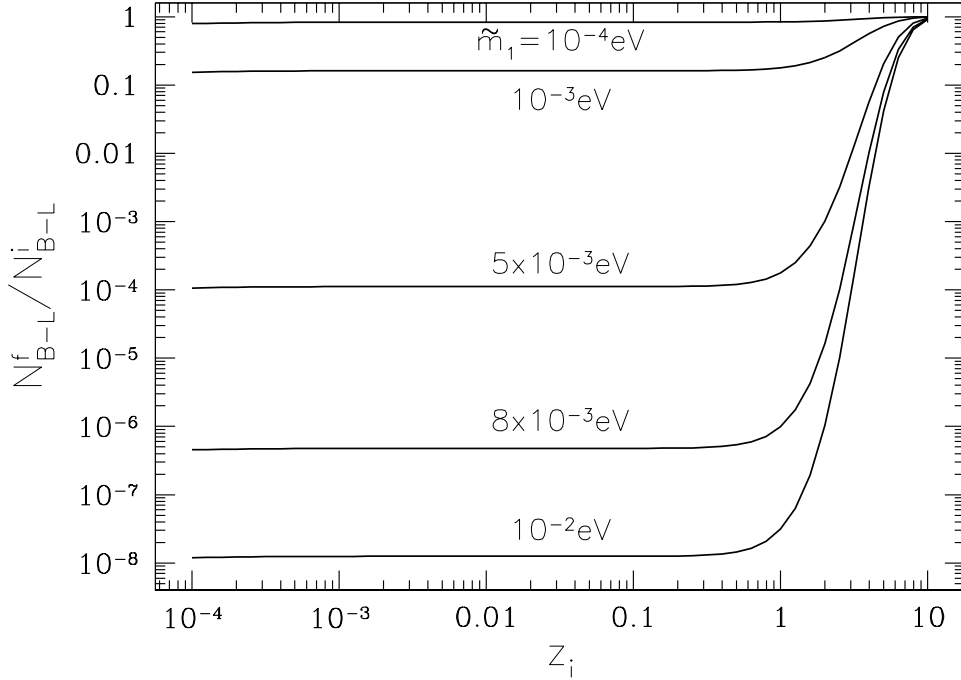
21

Figure 8: Washout factor as function of the initial temperature $z_i = M_1/T_i$ for different values of $\widetilde{m}_1$ and $M_1 = 10^8$ GeV; N_1-top scatterings are neglected.

For small and large values of z_i, respectively, analytic expressions are given by

$$\omega^{(3)}(z_i) = \begin{cases} \exp\left\{-\frac{\alpha_u}{2\zeta(3)}\frac{\widetilde{m}_1}{m_*}\left(\ln\left(4a_\phi\right)-1\right)\right\}, z_i < 1 \\ \exp\left\{-\frac{\alpha_u}{2\zeta(3)}\frac{\widetilde{m}_1}{m_*}\sqrt{\frac{2z_i}{\pi}}e^{-z_i}\left(\ln\left(\frac{a_\phi}{z_i^2}\right)\left(\frac{11}{8}+z_i\right)+\frac{5}{8}-z_i\right)\right\}, z_i > 1, \end{cases} \tag{67}$$

where $\alpha_u = g_t^2/(4\pi)$ and $a_\phi = M_1^2/m_\phi^2$.

The total washout factor

$$\omega(z_i) = \frac{N_{B-L}^f}{N_{B-L}^i} = \omega^{(1)}(z_i)\omega^{(2)}(z_i)\omega^{(3)}(z_i) \tag{68}$$

depends exponentially on the parameters $\widetilde{m}_1$ ($\omega^{(1)},\omega^{(3)}$) and $M_1\overline{m}^2$ ($\omega^{(2)}$). For not too large M_1 and not too small z_i (cf. Figs. (8)-(10)), $\omega^{(2)} \simeq 1$ whereas $\omega^{(1)}$ reaches a plateau for $z_i \leq 1$ at

$$\omega^{(1)}(z_i) \simeq \exp\left(-\frac{3\pi}{4\zeta(3)}\frac{\widetilde{m}_1}{m_*}\right). \tag{69}$$

At smaller values of z_i, and correspondingly higher temperatures T_i, eventually $\omega^{(2)}$ decreases rapidly. When T_i reaches M_2, the mass of N_2, a new plateau will be reached. The larger M_1, the larger the value of z_i where the decrease of $\omega^{(2)}$ sets in. This behaviour is
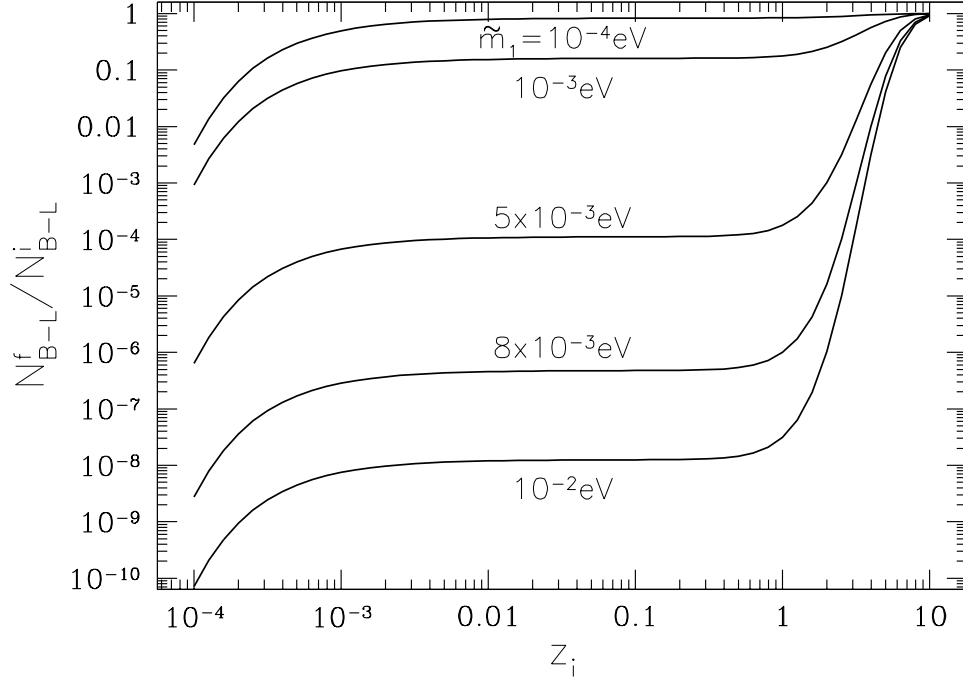
22

Figure 9: Washout factor as function of the initial temperature $z_i = M_1/T_i$ for different values of $\widetilde{m}_1$ and $M_1 = 10^{10}$ GeV; N_1-top scatterings are neglected.
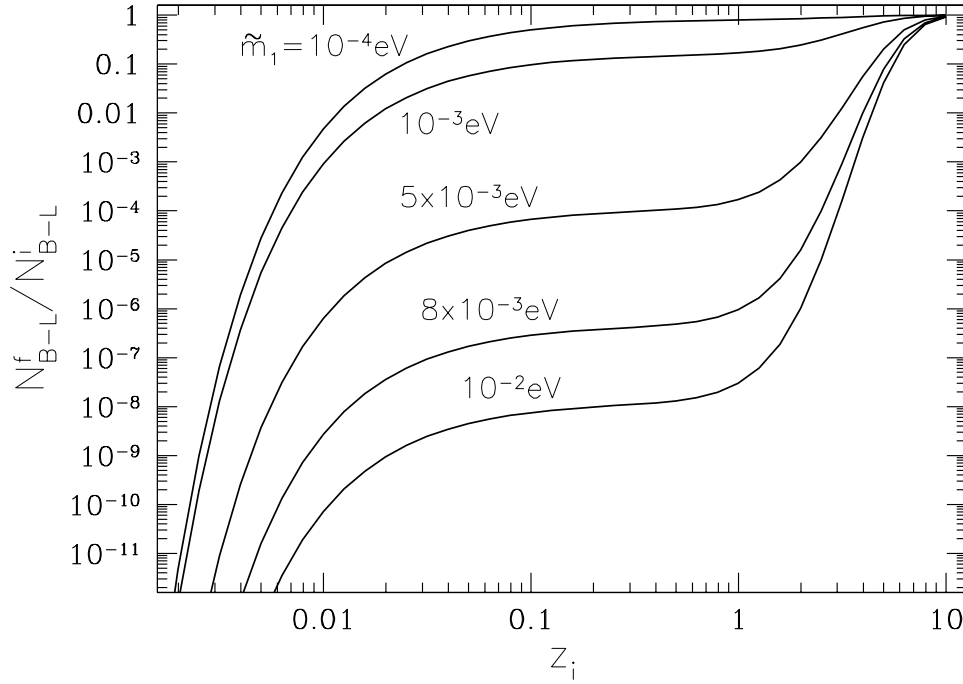

Figure 10: Washout factor as function of the initial temperature $z_i = M_1/T_i$ for different values of $\widetilde{m}_1$ and $M_1 = 10^{12}$ GeV; N_1-top scatterings are neglected.
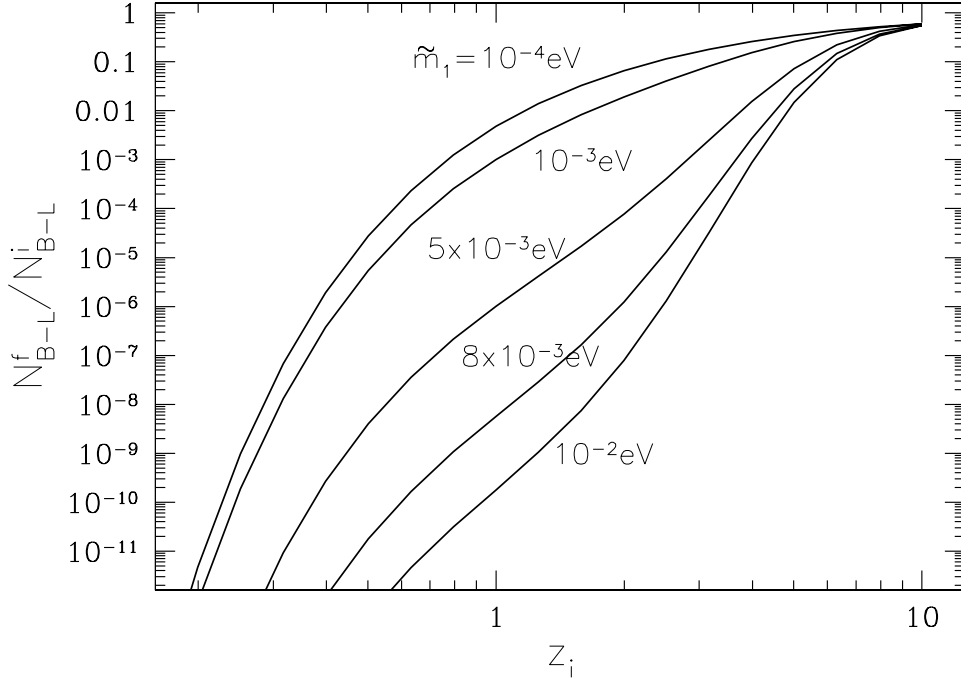
Figure 11: Washout factor as function of the initial temperature $z_i = M_1/T_i$ for different values of $\widetilde{m}_1$ and $M_1 = 10^{14}$ GeV; N_1-top scatterings are neglected.

clearly visible in Figs. (8)-(10). At very large M_1, the decrease of $\omega^{(2)}$ is effective already at large values of z_i (cf. Fig. (11)).

The factor $\omega^{(3)}$ is very sensitive to the value of a_ϕ, i.e. the choice of the infrared cutoff m_ϕ. For $m_\phi = 1$ TeV, $\omega^{(3)}$ significantly improves the washout of $\omega^{(1)}\omega^{(2)}$, but it does not change the qualitative picture. This is illustrated by Fig. (12) where the cases with and without N_1-top scatterings are compared. On the other hand, for $m_\phi \sim M_1$, $\omega^{(3)}$ is always negligible compared to $\omega^{(1)}$. The issue of the correct choice of the infrared cutoff is theoretically not yet settled. There is a corresponding, though less important uncertainty in the generation of the baryon asymmetry for small values of $\widetilde{m}_1$ [39]. The washout factors $\omega^{(1)}\omega^{(2)}$ shown in Figs. (8)-(11) can be regarded as conservative upper bounds on the full washout factors $\omega = \omega^{(1)}\omega^{(2)}\omega^{(3)}$.

It is remarkable that the washout of an initial asymmetry at $z_i \sim 1$, i.e. $T_i \sim M_1$, becomes very efficient for $\widetilde{m}_1 \geq m_* \simeq 10^{-3}$ eV. Since the efficiency increases exponentially with increasing $\widetilde{m}_1$, already at $\widetilde{m}_1 = 5 \times 10^{-3}$ eV one has $\omega(z_i = 1) < 10^{-4}$. Hence, for neutrino masses of order or larger than $\sqrt{\Delta m_{\mathrm{sol}}^2}$, $\Delta L = 1$ processes are very likely to erase any previously generated baryon asymmetry to a level below the asymmetry produced by leptogenesis. As shown in [9], for these values of $\widetilde{m}_1$ the final asymmetry is
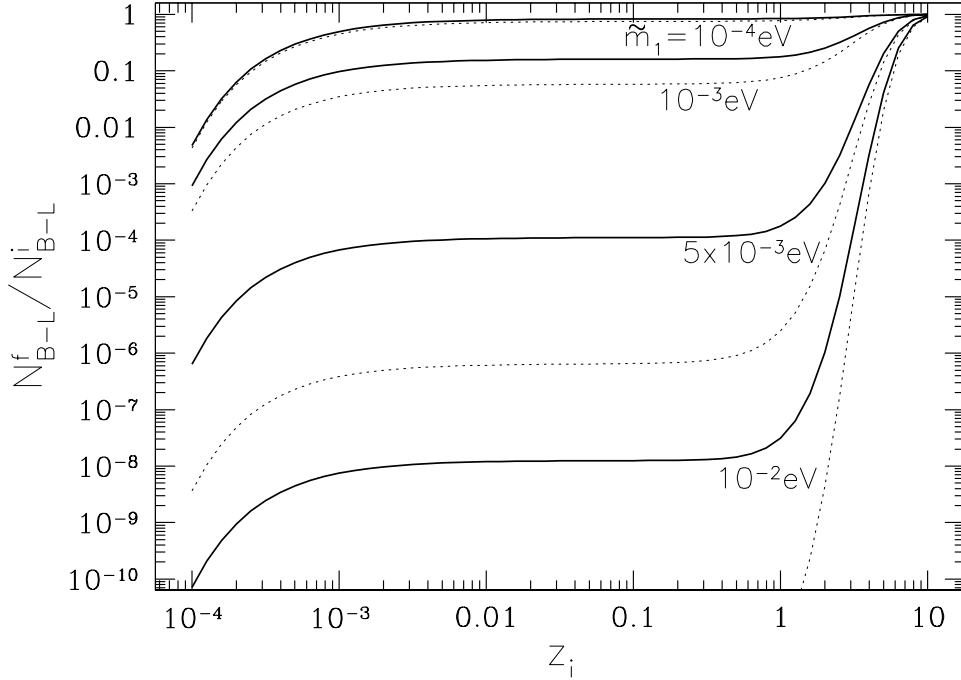
24

Figure 12: Comparison of the washout factors as function of $z_i = M_1/T_i$ without (full line) and with (dashed line) N_1-top scatterings; $M_1 = 10^{10}$ GeV.

also independent of the initial N_1 abundance. Hence, a complete independence of initial conditions is achieved.

6 Summary

We have extended our previous work on the minimal version of thermal leptogenesis where interactions of N_1, the lightest of the heavy Majorana neutrinos, are the dominant source of the baryon asymmetry. Based on the seesaw mechanism, we have derived an improved upper bound on the CP asymmetry ε_1, which depends on M_1, the mass of N_1, the light neutrino masses m_1 and m_3, and the effective neutrino mass $\widetilde{m}_1$. Given the two mass splittings $\Delta m^2_{\mathrm{atm}}$ and $\Delta m^2_{\mathrm{sol}}$, the neutrino masses m_1 and m_3 can depend on the absolute neutrino mass scale $\overline{m}$ in two ways, corresponding to normal and inverted mass hierarchy, respectively.

From the numerical solution of the Boltzmann equations we have obtained an upper bound on all light neutrino masses of 0.12 eV, which holds for normal as well as inverted neutrino mass hierarchy. This is about a factor of two below the recent upper bound of 0.23 eV obtained by MAP [50]. The leptogenesis bound is remarkably stable with respect

to changes of η_B^{CMB}, $\Delta m^2_{\mathrm{atm}}$, the effect of supersymmetry, and theoretical uncertainties of η_B^{max}. Quasi-degenerate neutrinos are only allowed if the CP asymmetry is strongly enhanced by a degeneracy of the heavy Majorana neutrinos. For instance, in order to relax the upper bound to 0.4 eV, degeneracies $\Delta M_{21}/M_1$, $\Delta M_{31}/M_1 \lesssim 10^{-3}$ are required.

We have also studied the washout of a large, pre-existing $B - L$ asymmetry. It is very interesting that a washout by several orders of magnitude takes place at temperatures T close to M_1, if the effective neutrino mass $\widetilde{m}_1$ is larger than the equilibrium mass $m_* \simeq 10^{-3}$ eV. All memory of the initial conditions is then erased.

We conclude that for neutrino masses in the range from 10^{-3} eV to 0.1 eV leptogenesis naturally explains the observed baryon asymmetry, independent of possible other pre-existing asymmetries. It is very remarkable that the data on solar and atmospheric neutrinos indicate neutrino masses precisely in this range.

References

[1] A. D. Sakharov, JETP Lett. **5** (1967) 24

[2] M. Yoshimura, Phys. Rev. Lett. **41** (1978) 281;
A. Y. Ignatev, N. V. Krasnikov, V. A. Kuzmin, A. N. Tavkhelidze, Phys. Rev. **D 76** (1978) 436

[3] D. Toussaint, S. B. Treiman, F. Wilczek, A. Zee, Phys. Rev. **D 19** (1979) 1036;
S. Weinberg, Phys. Rev. Lett. **42** (1979) 850;
M. Yoshimura, Phys. Lett. **B 88** (1979) 294;
S. Dimopoulos, L. Susskind, Phys. Rev. **D 18** (1978) 4500

[4] G. t'Hooft, Phys. Rev. Lett. **37** (1976) 8

[5] V. A. Kuzmin, V. A. Rubakov, M. E. Shaposhnikov, Phys. Lett. **B 155** (1985) 36

[6] T. Yanagida, in *Workshop on Unified Theories*, KEK report 79-18 (1979) p. 95;
M. Gell-Mann, P. Ramond, R. Slansky, in *Supergravity* (North Holland, Amsterdam, 1979) eds. P. van Nieuwenhuizen, D. Freedman, p. 315

[7] M. Fukugita, T. Yanagida, Phys. Lett. **B 174** (1986) 45

[8] E. W. Kolb, M. S. Turner, *The Early Universe*, Addison-Wesley, New York, 1990

[9] W. Buchmüller, P. Di Bari, M. Plümacher, Nucl. Phys. **B 643** (2002) 367

[10] K. Hamaguchi, H. Murayama, T. Yanagida, Phys. Rev. **D 65** (2002) 043512

[11] S. Davidson, A. Ibarra, Phys. Lett. **B 535** (2002) 25

[12] W. Buchmüller, P. Di Bari, M. Plümacher, Phys. Lett. **B 547** (2002) 128

[13] J. A. Casas, A. Ibarra, Nucl. Phys. **B 618** (2001) 171

[14] M. Flanz, E. A. Paschos, U. Sarkar, Phys. Lett. **B 345** (1995) 248; Phys. Lett. **B 384** (1996) 487 (E)

[15] L. Covi, E. Roulet, F. Vissani, Phys. Lett. **B 384** (1996) 169

[16] W. Buchmüller, M. Plümacher, Phys. Lett. **B 431** (1998) 354

[17] J. Ellis, M. Raidal, Nucl. Phys. **B 643** (2002) 229

[18] H. V. Klapdor-Kleingrothaus, Nucl. Phys. Suppl. **100** (2001) 350

[19] F. Feruglio, A. Strumia, F. Vissani, Nucl. Phys. **B 637** (2002) 345; hep-ph/0201291

[20] M. Fujii, K. Hamaguchi, T. Yanagida, Phys. Rev. **D 65** (2002) 115012

[21] M. Shiozawa at Neutrino 2002,
http://neutrino2002.ph.tum.de/pages/transparencies/shiozawa/index.html

[22] KamLAND Collaboration, K. Eguchi et al., hep-ex/0212021

[23] H. Fritzsch, Z. Xing, Prog. Part. Nucl. Phys. **45** (2000) 1

[24] A. Pilaftsis, Int. J. Mod. Phys. **A 14** (1999) 1811

[25] J. Ellis, M. Raidal, T. Yanagida, Phys. Lett. **B 546** (2002) 228

[26] G. C. Branco et al., hep-ph/0211001

[27] I. Dorsner, S. M. Barr, Nucl. Phys. **B 617** (2001) 493

[28] G. Altarelli, F. Feruglio, hep-ph/0206077

[29] W. Buchmüller, M. Plümacher, Phys. Lett. **B 389** (1996) 73

[30] J. Sato, T. Yanagida, Phys. Lett. **B 430** (1998) 127

[31] N. Irges, S. Lavignac, P. Ramond, Phys. Rev. **D 58** (1998) 035003

[32] C. D. Frogatt, H. B. Nielsen, Nucl. Phys. **B 147** (1979) 277

[33] W. Buchmüller, D. Wyler, Phys. Lett. **B 521** (2001) 291

[34] S. F. King, Nucl. Phys. **B 576** (2000) 85

[35] W. Buchmüller, T. Yanagida, Phys. Lett. **B 302** (1993) 240

[36] M. A. Luty, Phys. Rev. **D 45** (1992) 455

[37] M. Plümacher, Z. Phys. **C 74** (1997) 549

[38] M. Plümacher, Nucl. Phys. **B 530** (1998) 207

[39] R. Barbieri, P. Creminelli, A. Strumia, N. Tetradis, Nucl. Phys. **B 575** (2000) 61;
hep-ph/9911315v3

[40] S. Yu. Khlebnikov, M. E. Shaposhnikov, Nucl. Phys. **B 308** (1988) 885;
     J. A. Harvey, M. S. Turner, Phys. Rev. **D 42** (1990) 3344

[41] P. de Bernardis et al., Astrophys. J. **564** (2002) 559

[42] C. Pryke et al., Astrophys. J. **568** (2002) 46

[43] W. Buchmuller, P. Di Bari and M. Plumacher, in preparation.

[44] http://map.gsfc.nasa.gov/m_mm/ms_status.html

[45] http://astro.estec.esa.nl/Planck/

[46] D. Michael at Neutrino 2002,
     http://neutrino2002.ph.tum.de/pages/transparencies/michael/index.html

[47] S. Katsenavas at Neutrino 2002,
     http://neutrino2002.ph.tum.de/pages/transparencies/katsanevas/index.html

[48] KATRIN Collaboration, A. Osipowicz et al., hep-ex/0109033

[49] A. Erdélyi, W. Magnus, F. Oberhettinger and F. G. Tricomi, *Higher Transcendental
     Functions, vol. II* (McGraw-Hill Book Company, 1953)

[50] WMAP Collaboration, D. N. Spergel et al., astro-ph/0302209